

Validation of the Integrated Biosphere Simulator over Canadian deciduous and coniferous boreal forest stands

Mustapha El Maayar,¹ David T. Price,¹ Christine Delire,² Jonathan A. Foley,²
T. Andrew Black,³ and Pierre Bessemoulin⁴

Abstract. Data collected during the Boreal Ecosystem–Atmosphere Study (BOREAS) at four different forest stands were used to test surface energy and carbon fluxes simulated by the Integrated Biosphere Simulator (IBIS). These stands included deciduous and conifer species and were located in both the BOREAS northern and southern study areas. Two runs were made: one using the original IBIS model and the other using a version modified to consider an organic soil layer (OSL) covering the mineral soil surface. Results show that the inclusion of the OSL substantially improved the simulation of soil heat flux, as well as of temperature and moisture in the topmost soil layer. Simulations show that latent and sensible heat fluxes, and net ecosystem exchange of carbon, were not affected appreciably by the presence of a thin (10 cm or less) OSL covering the forest floor. With a thick (50 cm) OSL, however, simulation of latent heat flux and net ecosystem exchange of carbon was substantially improved. Consideration of the OSL in the model also led to better simulation of the onsets of soil thawing. Correct estimation of heat diffusion to deep soil through thick organic layers requires a parameterization that accounts for the state of the organic material decomposition. Simulations presented here also show the necessity for using detailed information on soil physical properties for better evaluation of model performance.

1. Introduction

Characteristics of vegetated terrestrial surfaces influence weather, climate, and atmospheric composition through their effects on exchanges of radiation, heat, water, momentum, and carbon [Shukla and Mintz, 1982; Pielke *et al.*, 1997; Hogg *et al.*, 2000]. For the last three decades, considerable modeling effort has been invested in understanding these influences. During this time, land surface parameterization models developed primarily for implementation in Atmospheric General Circulation Models (AGCMs) have evolved from simple aerodynamic bulk transfer formulae and uniform prescriptions of surface parameters (e.g., albedo, aerodynamic roughness, soil moisture) [Manabe and Bryan, 1969; Schneider and Dickinson, 1974; Manabe and Wetherald, 1987] to more realistic representations of terrestrial biophysical processes (e.g., SiB of Sellers *et al.* [1986] and CLASS of Verseghy *et al.* [1993]). More recently, process-based biophysical models have also taken into account photosynthesis and plant water relations to provide a more internally consistent description of the coupled fluxes of energy, water, and carbon (e.g., the revised land surface scheme

SiB2 of Sellers *et al.* [1996], the revised ISBA of Calvet *et al.* [1998], and Dynamic Global Vegetation Models (DGVMs) such as the Integrated Biosphere Simulator (IBIS) of Foley *et al.* [1996]).

The formulations of such models are necessarily complex yet must include numerous approximations and assumptions (because many of the processes are themselves complex and remain poorly understood). For this reason, an international Project for Intercomparison of Land Surface Parameterization Schemes (PILPS) was initiated [Henderson-Sellers and Brown, 1992], in which different land surface parameterizations were compared with observed flux data. Results involving 23 land surface schemes were reported by Henderson-Sellers *et al.* [1996] and Chen *et al.* [1997]. As pointed out by Delire and Foley [1999], however, the PILPS study did not include data from any forested sites.

It is now fairly clear that the circumpolar boreal forest (of North America, Scandinavia, and northern Asia) plays an important (if not crucial) role in regulating atmospheric CO₂ content by acting as a carbon sink [Tans *et al.*, 1990; Gates, 1993; Ciais *et al.*, 1995; Sellers *et al.*, 1997]. It may yet prove to be just as important in controlling the global climate [e.g., Bonan *et al.*, 1992; Foley *et al.*, 1994; Pielke and Vidale, 1995; Hogg *et al.*, 2000]. Consequently, it is of considerable interest whether biospheric models such as IBIS, designed as dynamic vegetation schemes for use in AGCMs, can reproduce observed fluxes in this particular region, in addition to the general importance of validating them for different forest ecosystems. In the study reported here, the performance of IBIS operating in a stand-alone mode was investigated for different forests types located within the Boreal Ecosystem Atmosphere Study (BOREAS) region [Sellers *et al.*, 1997]. These forest sites, located both in the southern and the northern study areas (SSA and NSA, respectively), are known within the BOREAS liter-

¹Natural Resources Canada, Canadian Forest Service, Edmonton, Alberta, Canada.

²Center for Sustainability and the Global Environment, Institute for Environmental Studies, University of Wisconsin-Madison, Madison, Wisconsin.

³Department of Agroecology, University of British Columbia, Vancouver, British Columbia, Canada.

⁴Météo-France, Service Central d'Exploitation de la Météorologie, Toulouse, France.

Copyright 2001 by the American Geophysical Union.

Paper number 2001JD900155.
0148-0227/01/2001JD900155\$09.00

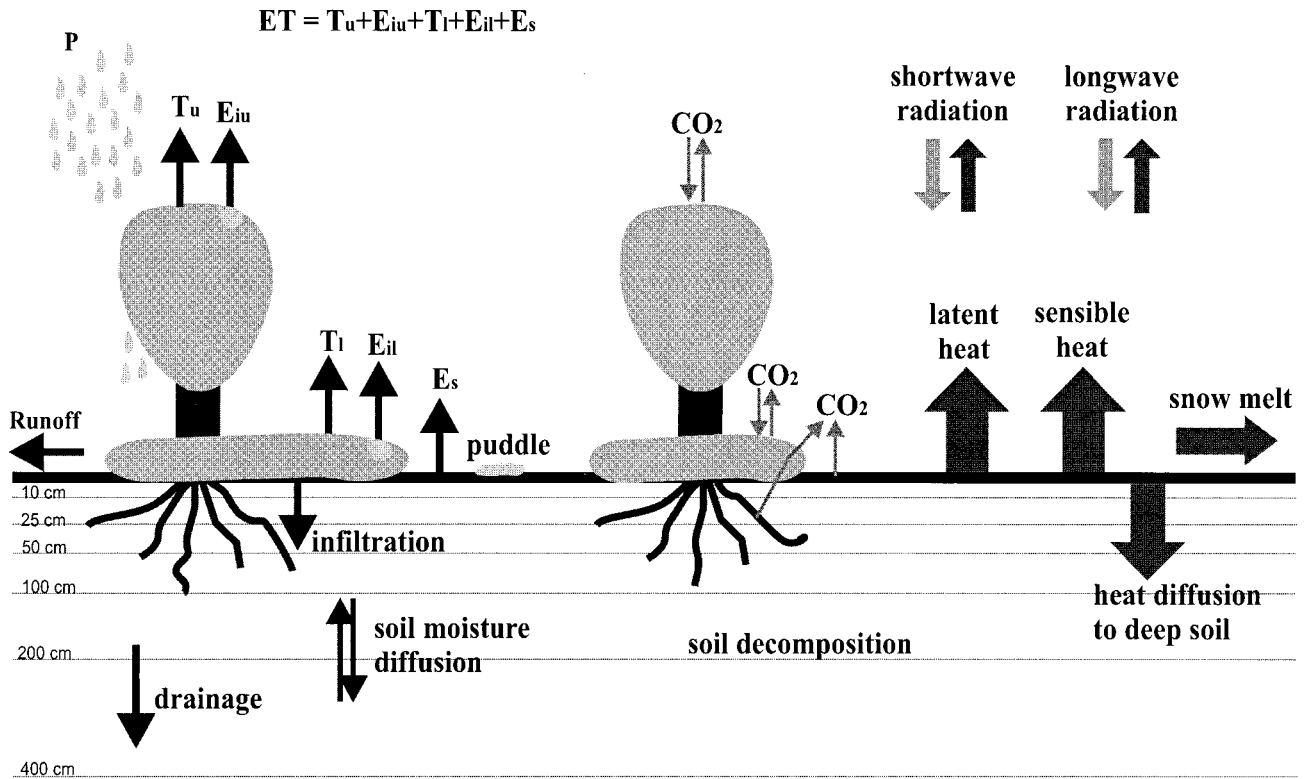


Figure 1. Schematic illustration of the water balance, the carbon balance, and the energy balance calculations performed by IBIS. The following terms of the terrestrial water and energy budgets are explicitly simulated: evapotranspiration (ET), which is the sum of transpiration (T_u and T_l), evaporation from the soil surface (E_s), evaporation of water intercepted by vegetation canopies (E_{iu} and E_{il}); runoff, soil water infiltration, subsurface drainage; latent, sensible, and soil heat fluxes; upward shortwave and longwave radiation; net carbon assimilation; autotrophic (root) and heterotrophic (microbes) respiration. Precipitation (P: rain + snow), downward shortwave and longwave radiation, and atmospheric CO_2 concentration are prescribed. The subscripts u and l refer to the upper and lower canopies, respectively.

ature as the northern old black spruce (NOBS), southern old jack pine (SOJP), southern old-aspen (SOA), and southern young aspen (SYA) stands. Within the North American boreal, forest dominated by black spruce (*Picea mariana* (Mill.) B.S.P.) is most common [Larson, 1980], although aspen (*Populus tremuloides* Michx.) is the dominant deciduous species. In the BOREAS region, jack pine (*Pinus banksiana* Lamb.) is the secondmost common coniferous species. The BOREAS data therefore provide an important basis for validating IBIS when applied to high-latitude forest ecosystems. Only when such studies have confirmed that the model is able to provide realistic responses to present-day climate for a range of ecosystems will it be appropriate to use it to assess effects of possible climatic changes on forest processes and distribution.

2. Model Description

Version 2.1 of IBIS [Kucharik *et al.*, 2000] was used in this study. This model is hierarchically organized to allow for explicit coupling among ecological, biophysical, and physiological processes operating at different timescales [Foley *et al.*, 1996]. Heat, momentum, and water exchanges are computed using the LSX land surface scheme model of Pollard and Thompson [1995]. LSX borrows its main structure from the SiB [Sellers *et al.*, 1986] and BATS [Dickinson *et al.*, 1986] models, simulating two vegetation layers (corresponding to upper and lower canopies), and six soil layers with horizon thicknesses of 0.1, 0.15,

0.25, 0.50, 1.0, and 2.0 m, respectively. IBIS simulates carbon exchange and stomatal regulation of both C_3 and C_4 plant species according to a semimechanistic approach based on physiological evidence [Farquhar *et al.*, 1980; Ball *et al.*, 1986; Collatz *et al.*, 1991, 1992]. Net ecosystem exchange (NEE) is computed as the difference between carbon taken up by the vegetation through gross (canopy-level) photosynthesis and carbon lost through plant respiration of foliage, wood, and roots and through microbial decomposition of litter and soil organic matter. For all the simulations reported here, vegetation was treated as “static” in the IBIS vegetation dynamics module; i.e., no change in stand structure was assumed to occur during the periods for which simulations were performed. Figure 1 provides a schematic description of the LSX land surface scheme as coupled with the photosynthetic model of Collatz *et al.* [1991] and the soil respiration model of Lloyd and Taylor [1994].

3. Data and Study Sites

Detailed descriptions of sites, instrumentation, and measurements are reported by Black and Nesic [1999] and Chen *et al.* [1999] for SOA; by Bessemoulin and Puech [1998] for SYA; by Baldocchi *et al.* [1997a, 1997b] for SOJP; and by Goulden *et al.* [1997] for NOBS. Measurements of turbulent fluxes of latent and sensible heat, and NEE were performed using the eddy correlation technique (referred to from here on as EC).

Table 1. Vegetation and Soil Parameters Used for the Simulations

		Forest Site			
		SOA	SYA	SOJP	NOBS
<i>Vegetation Parameters</i>					
Vegetation type	upper	trees	trees	trees	trees
	lower	shrubs		C3 grass	
Fractional vegetation cover	upper	0.8	0.9	0.8	0.9
	lower	0.8		0.8	
Vegetation height, m	upper	21.50	2.75	13.50	10.00
	lower	2.00		0.20	
Leaf area index (LAI)	upper	daily ^a	5.5	2.4	4.5
	lower	daily ^b		2.0	
Stem area index (SAI)	upper	0.4	0.4	0.2	0.6
V_{\max}^c	upper	30.0	30.0	25.0	25.0
	lower	27.5		25.0	
<i>Soil Parameters</i>					
Soil texture		silty loam	silty loam	sand	silty clay
Soil sand/silt/clay content, %		20/65/15	20/65/15	92/05/03	10/45/45
Soil depth, m		1.00	1.00	1.00	4.00
Organic layer thickness, m		0.08	0.08	0.05	0.5
Initial soil temperature, °C (by layer)		12.1/10.6/10.0/9.3	12.1/12.1/12.1/12.1	13.4/12.1/11.6/11.6	-5.9/-4.3/-3.5/-2.0/-0.49/-0.5
Initial soil moisture content, m ³ /m ³ (by layer)		0.58/0.58/0.47/0.37	0.16/0.23/.23/0.38	0.1/0.1/0.1/0.15	0.0
Initial soil ice content, m ³ /m ³		0.00	0.00	0.00	0.80
Soil porosity, m ³ /m ³	mineral soil	0.50	0.50	0.44	0.48
	organic soil	0.80	0.80	0.80	0.80
Field capacity, m ³ /m ³	mineral soil	0.33	0.33	0.09	0.39
	organic soil	0.60	0.60	0.60	0.60
Wilting point, m ³ /m ³	mineral soil	0.13	0.13	0.03	0.25
	organic soil	0.20	0.20	0.20	0.20
Saturated hydraulic conductivity, m/d	mineral soil	0.25	0.48	1.46	0.46
	organic soil	0.25	0.48	1.46	0.46
Saturated air entry potential, m	mineral soil	0.21	0.21	0.07	0.34
	organic soil	0.21	0.21	0.07	0.34
Soil b parameter	mineral soil	4.70	4.70	1.70	7.90
	organic soil	4.70	4.70	1.70	7.90
Total soil carbon, kg-C/m ²		3.60	3.60	1.42	4.18
Total litter carbon, kg-C/m ²		1.11	1.11	0.67	0.48

^aLAI_{max} (upper canopy) is 2.

^bLAI_{max} (lower canopy) is 2.3.

^c V_{\max} is the maximum Rubisco capacity at 15°C of the top leaf. Their values were taken from *Kucharik et al.* [2000].

All observed data were recorded at half-hourly intervals. Only hourly data were used; however, data collected on the half hours were deleted except for precipitation where half hourly data were added to obtain hourly data (mm h⁻¹). Tests showed that no pertinent information was lost using hourly in place of half-hourly observations.

The SOA site was an extensive 70-year old stand, dominated by aspen, located in the BOREAS Southern Study Area (SSA) at ~53.7°N, 106.2°W. Average tree height was ~21.5 m. The understory vegetation was composed mainly of hazelnut (*Corylus cornuta* Marsh) ~2 m tall. The soil is predominantly an Orthic Luvisol with an 8–10 cm deep surface organic layer [Black *et al.*, 1996]. Data used in this study were collected during the 1996 field campaign and cover the period June 1 to December 31.

The SYA site was also located in the SSA, with approximate coordinates of 53.39°N, 105.20°W. The stand was dominated by aspen, with very high stem density (~10 stems m⁻²) and a mean tree height of 2.75 m. Soils ranged from gray wooded to degraded black, classified in the brunisolic, gleysolic, chernoz-

emic, luvisolic, and organic soil orders. Data reported here were obtained in the period July 17 to August 16, 1994. No NEE measurements were available for this site.

The SOJP site was located in the SSA region at 53.55°N, 104.41°W. Dominated by jack pine, with a mean canopy height of 13.5 m, the stand extended for over one kilometre from the instrument tower in all directions. Understory shrubs were sparse, consisting of isolated patches of alder (*Alnus crispa*). Ground cover was extensive however, including bearberry (*Arctostaphylos uva-ursi*), bog cranberry (*Vaccinium vitis-idaea*), and lichens (*Cladina* spp.). Soil was a coarse textured sand, classified as a degraded Eutric Brunisol/Orthic Eutric Brunisol. Data used in this study were obtained for the period July 1 to September 16, 1994.

The NOBS site was located in the BOREAS Northern Study Area (NSA) at 55.88°N, 98.48°W, surrounded by a black spruce-dominated forest of varying stature extending for several kilometers in all directions [Goulden *et al.*, 1997]. Mean tree height was ~10 m. Soils in this area consist of organics, clays, and some sandy deposits. Data used in this study were

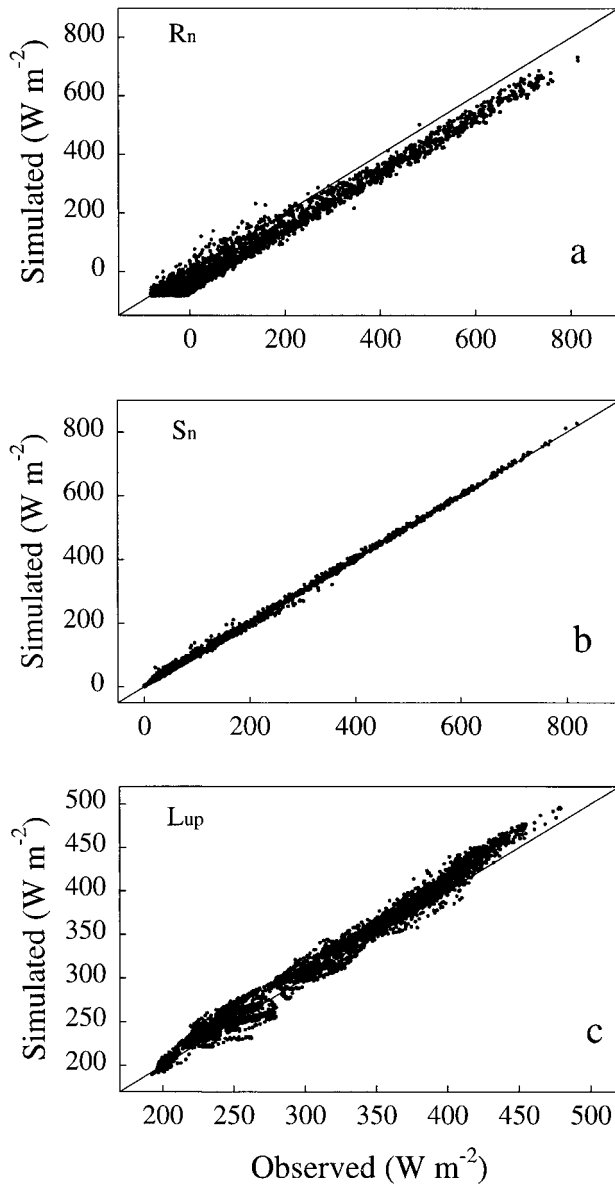


Figure 2. Observed and simulated: (a) net radiation (R_n), (b) net shortwave radiation (S_n), and (c) upward longwave radiation (L_{up}) at old aspen site during the period June 1 to December 31 1996.

obtained for the period April 1 to October 9, 1996. No soil heat flux measurements were available at this site.

For each hourly time step, IBIS simulated the energy and C balances using the following forcing variables: air temperature, hourly total precipitation, wind speed, humidity, incoming short-wave and long-wave radiation, and surface air pressure. Incoming long-wave radiation, whenever missing, was estimated using the formula of *Satterlund* [1979]. Occasional data gaps were filled using mesonet station data [*Shewchuk*, 1997]. In addition, site-specific regression equations, derived from measured data, that expressed net radiation as a function of incoming shortwave radiation, were used to fill very occasional gaps in shortwave radiation time series.

The data used to initialize the model are shown in Table 1. Soil temperature data were available for all sites. For the SOA site, measured soil moisture was used to initialize the model.

For the NOBS site, initial soil water content was assumed equal to porosity and all in the form of ice. Initial soil moisture content values at the SYA and SOJP sites were taken from *Cuenca et al.* [1997] and *Nijssen et al.* [1997], respectively.

Soil textures for SOA and SOJP sites were classified as silty loam and sandy, respectively, based on data given by *Cuenca et al.* [1997] (Table 1). For the NOBS site, soil texture data were taken from the global data set used in large-scale simulations with IBIS [*Foley et al.*, 1996]. Soil at the SYA site was assumed to have the same texture as that found at the SOA site. For all SSA sites, soil hydraulic properties were taken from *Nijssen et al.* [1997] and *Cuenca et al.* [1997], with soil depth set to 1 m, following data from *Clayton et al.* [1977]. Fractional vegetation cover and leaf area index (LAI) for SOJP and NOBS, and stem area index values, were taken from *Kimball et al.* [1997], *Nijssen et al.* [1997], and *Gower et al.* [1997], respectively. Leaf area index at SYA was assumed equal to that reported for SOA by *Black et al.* [1996] for the period of the simulation, as also reported by R. D. Pyles et al. (personal communication, 1999). Daily changes in LAI at SOA, as reported by *Chen et al.* [1999], were approximated using a third-order polynomial function. Root profiles were as given by *Nijssen et al.* [1997] for SOJP and NOBS and as given by *Jackson et al.* [1996] for SOA and SYA. Total soil carbon and total litter carbon values, were taken from *Gower et al.* [1997] and *Steele et al.* [1997].

4. Comparison of Observed and Simulated Data

Two series of simulations were performed for each forest stand. The first series was carried out using only mineral soil texture classes, as used in IBIS2.1 simulations at the global scale by *Kucharik et al.* [2000]. For much of the Canadian boreal forest zone, however, particularly those vegetation communities dominated by aspen and spruce, an organic layer covers the surface [*Clayton et al.*, 1977]. Typically, this layer is deeper in the northern regions because decomposition rates are normally lower than in the warmer conditions farther south. Hence, for our second series of simulations, an organic soil layer was introduced into the model, with thickness fixed according to observations made by *Black et al.* [1996] for the SOA site, by *Baldocchi et al.* [1997a] for SOJP, and by *Clayton et al.* [1977] for NOBS (see Table 1). For the SYA site we used the same thickness as that reported for SOA. At the SOA, SYA, and SOJP sites, only the top layer of the six model layers was treated as organic, but at NOBS the top four layers were all treated as organic, replacing the corresponding mineral soil layers. Moreover, when presence of organic soil was simulated, surface albedo was set equal to 0.1 (i.e., it was treated as a moist dark soil as defined in Table 6.4 of *Brutsaert* [1982]). Mineral soil albedos were computed by the model as a function of sand, silt, and clay fractions following *Dickinson et al.* [1986].

Heat capacity of dry organic material ($0.58 \text{ MJ m}^{-3} \text{ K}^{-1}$) and thermal conductivity ($0.06 \text{ W m}^{-1} \text{ K}^{-1}$) were taken from *Guyot* [1997]. Because of the lack of information on the particle size distribution (or degree of decomposition) of the organic matter layers at the study sites, saturated hydraulic conductivity and the soil b parameter (i.e., the exponent for the Campbell moisture release equation [*Campbell and Norman*, 1998]) were assumed to be the same in both sets of simulations: i.e., with and without the simulated soil organic layer. Data for saturated hydraulic conductivities at each site were obtained from *Cuenca* [1997].



Figure 3. Simulated hourly above-canopy fluxes plotted against data observed at the old aspen site during the period June 1 to December 31, 1996. (a) Sensible heat flux assuming presence of mineral soil only, (b) mineral soil with surface organic layer. (c) Latent heat flux assuming presence of mineral soil only, (d) mineral soil with surface organic layer. (e) Soil heat flux during the period when trees are in leaf, (f) when trees are leafless. Dark dots indicate that the run assumed the presence of mineral soil only and light triangles indicates that the run assumed the presence of mineral soil with surface organic layer. (g) Net ecosystem exchange (NEE) assuming presence of mineral soil only, and (h) mineral soil with surface organic layer. Carbon flux (NEE) flux is positive toward the atmosphere.

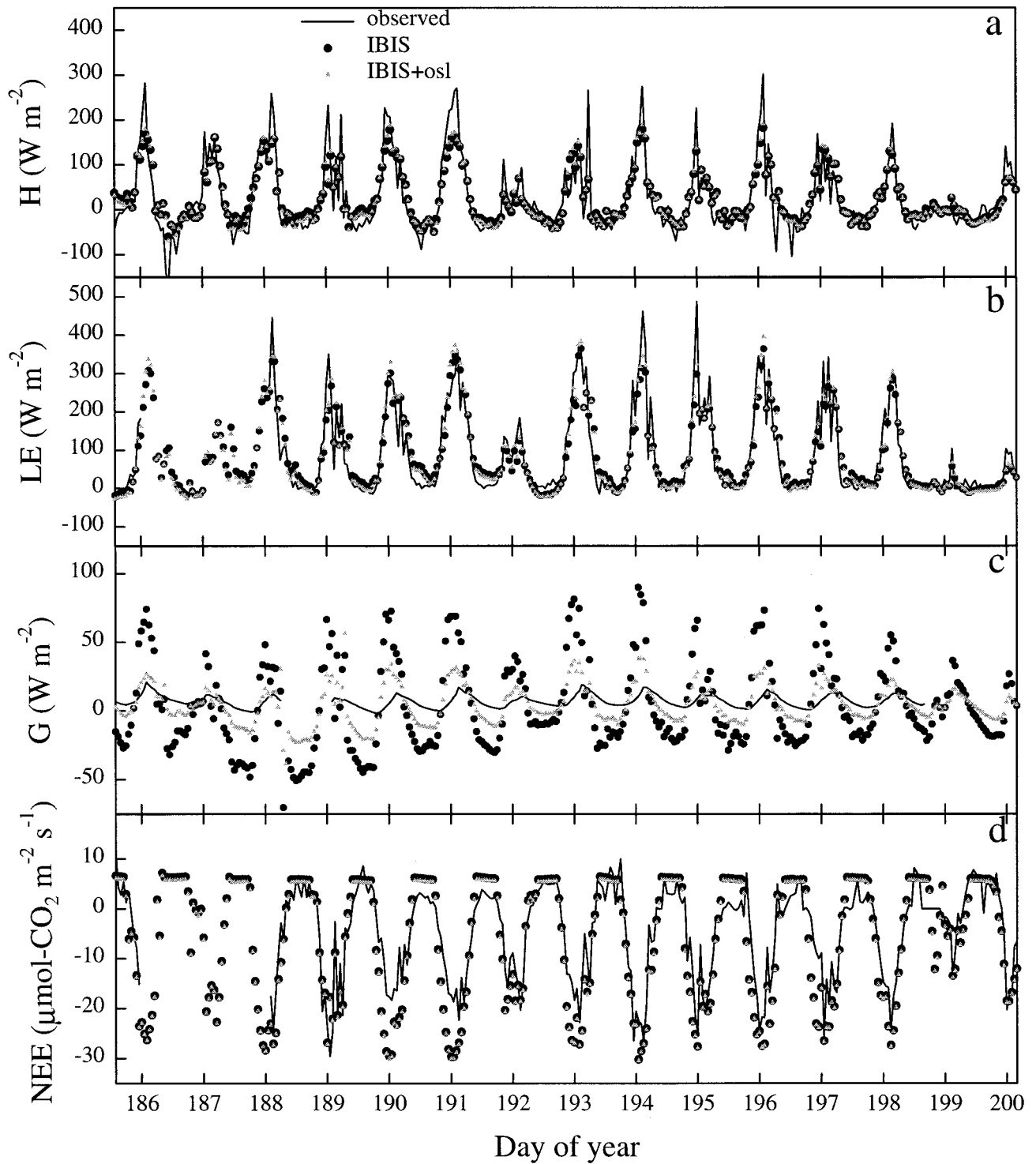


Figure 4. Observed and simulated diurnal variation of: (a) sensible heat flux, (b) latent heat flux, (c) soil heat flux, and (d) net ecosystem exchange at old aspen site. Dots indicate assumed presence of mineral soil only; gray triangles indicate assumed presence of mineral soil with surface organic layer. Carbon flux (NEE) is positive toward the atmosphere.

5. Results

5.1. SOA Site

Simulated and observed radiation and flux data are shown in Figures 2, 3, and 4. The agreement between observed and

simulated net shortwave radiation (S_n) is high (Figure 2b), suggesting that the parameterization of surface albedo was fairly accurate. Agreement between observed and simulated fluxes of net radiation (R_n), and upward longwave radiation (L_{up}) is also reasonable, although R_n is slightly underesti-

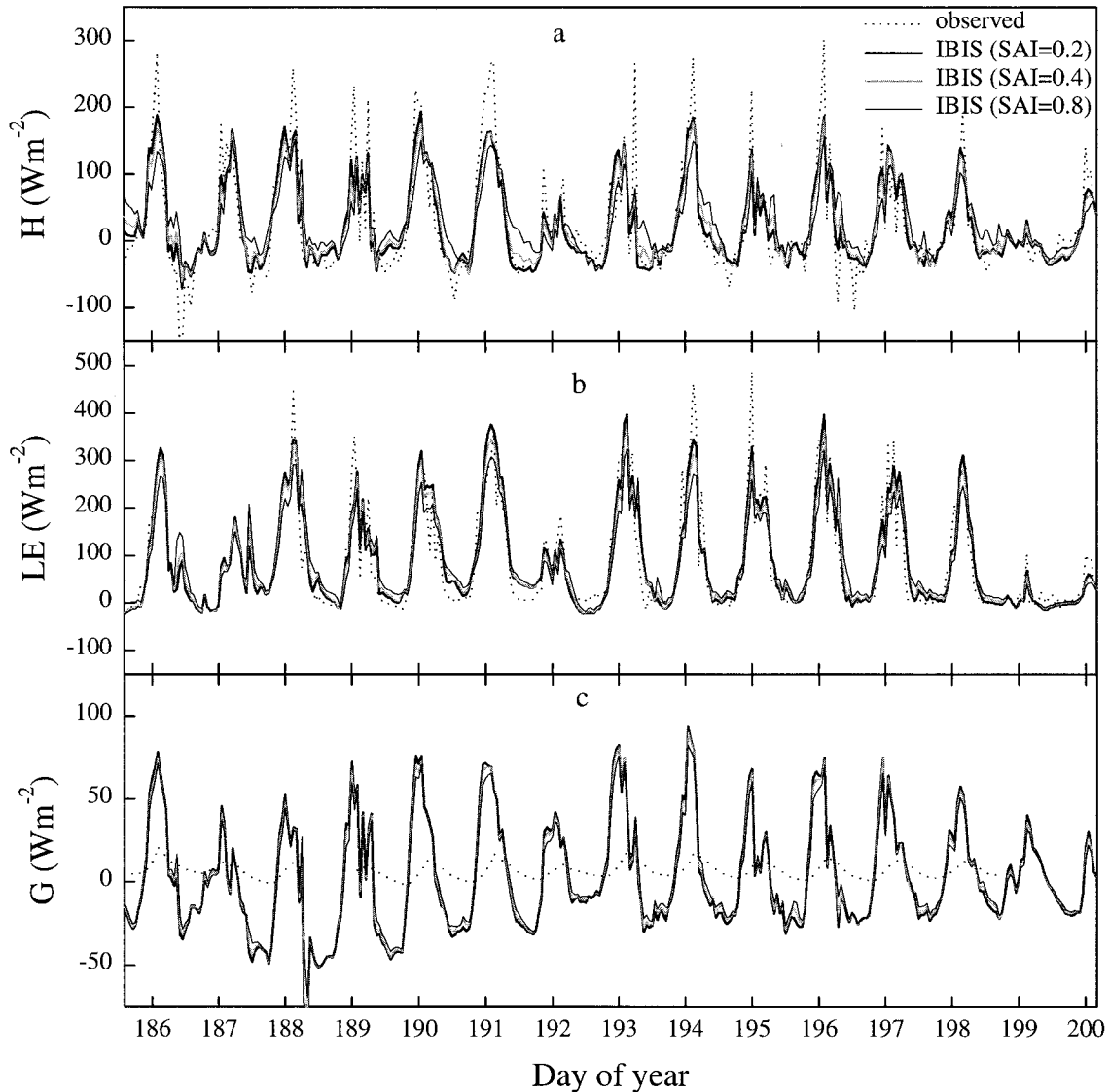


Figure 5. Sensitivity of simulated energy fluxes to different input values of stem area index (SAI), at old aspen site: (a) sensible heat flux, (b) latent heat flux, and (c) soil heat flux.

ated owing to overestimation of L_{up} (Figure 2c). The latter results from overestimation of surface soil temperature (Figures 5a and 5b).

Agreement between observed and simulated latent heat flux (LE) (Figures 3c, 3d, and 4b) is higher than for sensible heat flux (H) (Figures 3a, 3b, and 4a) and soil heat flux (G) (Figures 3e, 3f, and 4c). This bias obtained in the simulation of H causes a temporary imbalance, mainly around midday, in the total heat flux. Two other simulation studies reported a similar, but larger bias in the LSX model [Pollard and Thompson, 1995; Delire and Foley, 1999]. Analyzing the performance of LSX in tropical forests, Pollard and Thompson [1995] suggested that the heat imbalance was caused by exaggerated heat storage in trunks and stems (estimated from stem area index, SAI) and released mainly by evaporation during the night. To test this hypothesis, we ran the model for different values of stem area (Figure 5). Doubling the SAI increased the midday bias in both simulated sensible and latent heat fluxes, while halving the SAI led to a relative improvement in the simulation of LE as well as H (Figures 5a and 5b). Sensitivity of soil heat flux (G) to the

selected value of SAI was relatively minor (Figure 5c). A further development of this point is pursued in section 5.3 where measured canopy heat storage data were available for the SOJP site.

The model generally overestimates observed G (Figures 3e and 4c), a problem common to many land surface models, particularly when they are applied to forest sites [e.g., Shao and Henderson Sellers, 1996; Chen *et al.*, 1997; Delire and Foley, 1999; Bellisario *et al.*, 2000]. This evidently results from lack of consideration of the role of the organic layer usually covering forest floors. Indeed, after including an organic layer, referred to here as the IBIS + osl run (Figures 3e, 3f, and 4c), mean simulated G was much closer to the observed values, although it remained higher for daytime and lower for nighttime (Figure 4c). Poor numerical resolution of soil temperature near the surface is a common problem with land surface models, as explained by Betts *et al.* [1993] (working on surface parameterizations for the European Centre for Medium-Range Weather Forecasts) and by Chen *et al.* [1997] (who carried out a PILPS study involving 23 land surface schemes using data from the

Table 2. Averages and Standard Deviations of Observed and Simulated Fluxes^a

	Average Observed	IBIS	IBIS + osl	Standard Deviation Observed	IBIS	IBIS + osl	nb of Observations
<i>SOA Forest-SSA</i>							
R_n , $W m^{-2}$	84.31	44.45	47.39	187.74	175.94	175.66	5039
H , $W m^{-2}$	21.89	8.43	8.28	77.21	36.84	40.14	4632
LE , $W m^{-2}$	48.11	53.28	55.00	82.22	93.89	102.93	4268
Bowen ratio, H/LE	0.46	0.16	0.15	0.94	0.39	0.39	4268
G , $W m^{-2}$	0.82	-11.10	-9.53	6.51	40.00	25.41	4897
NEE-1, $\mu mol-CO_2 m^{-2} s^{-1}$	-2.95	-3.70	-4.01	7.92	10.22	10.20	2591
NEE-2, $\mu mol-CO_2 m^{-2} s^{-1}$	1.38	2.56	2.52	1.44	0.60	0.58	1672
NEE-3, $\mu mol-CO_2 m^{-2} s^{-1}$	-1.39	-1.45	-1.66	6.72	8.72	8.75	4263
<i>SYA Forest-SSA</i>							
R_n , $W m^{-2}$	153.57	136.54	138.35	223.24	236.56	235.25	696
H , $W m^{-2}$	13.81	29.12	29.21	49.46	39.49	41.41	676
LE , $W m^{-2}$	94.48	100.92	104.05	116.49	107.71	121.36	666
Bowen ratio, H/LE	0.15	0.29	0.28	0.42	0.37	0.34	666
G , $W m^{-2}$	2.44	6.41	5.07	15.07	40.31	19.91	696
<i>SOJP Forest-SSA</i>							
R_n , $W m^{-2}$	121.73	88.03	87.84	194.63	204.71	200.33	1755
H , $W m^{-2}$	61.32	52.08	56.85	110.59	85.98	92.16	1729
LE , $W m^{-2}$	47.84	32.75	29.44	64.61	66.20	73.72	1722
Bowen ratio, H/LE	1.28	1.59	1.93	1.71	1.30	1.25	1722
G , $W m^{-2}$	-1.40	2.14	1.51	18.20	33.62	14.79	1765
NEE, $\mu mol-CO_2 m^{-2} s^{-1}$	-0.43	-0.40	-0.78	4.59	1.68	1.93	1716
<i>NOBS Forest-NSA</i>							
R_n , $W m^{-2}$	124.03	87.09	87.23	202.93	216.25	215.58	4607
H , $W m^{-2}$	63.13	50.54	50.33	126.05	84.63	85.79	4344
LE , $W m^{-2}$	31.42	26.23	30.03	47.38	34.32	44.91	4322
Bowen ratio, H/LE	2.01	1.93	1.68	2.66	2.47	1.91	4322
G , $W m^{-2}$		7.60	4.09		31.40	14.90	
NEE, $\mu mol-CO_2 m^{-2} s^{-1}$	-0.45	0.21	-0.57	3.03	1.16	1.44	4350

^aIBIS + osl indicates that the first soil layer in IBIS was considered as organic for YA, OA, and OJP sites. Idem for OBS site but the four first soil layers was set as organic in this case. NEE-1 is the NEE for the period when trees are in leaf; NEE-2 is the NEE for the period when trees are leafless; and NEE-3 is the total NEE (NEE1 + NEE2). Depth of the soil organic layer used in the IBIS + osl simulation is: 8 cm for SOA and SYA, 5 cm for SOJP, and 50 cm for NOBS.

Cabauw grassland site). This causes an amplification of soil heat fluxes and a delay of turbulent fluxes.

Simulated and observed NEE data are shown in Figures 3g, 3h, and 4d. We adopted the convention that NEE is positive when the net flux is toward the atmosphere. Agreement between the simulation and measurements is lower around noon than at other times of day. *Delire and Foley* [1999] reported a similar problem when comparing results of their simulation for a grassland site with data from the FIFE experiment [*Verma et al.*, 1992]. Figure 4d also shows that the model generally overestimates nighttime respiration. Recent analyses by *Baldocchi et al.* [1998] and *Lee* [1998] on the reliability of EC measurements of carbon exchange between the surface and the atmosphere in forests may help to explain these results. By analyzing the conservation equation of CO_2 [*Baldocchi et al.*, 1998, Equation (1)]. These authors suggest that the conventional analysis of EC data may neglect an important advective effect in forests under stable conditions, occurring particularly at night. Although there is some controversy surrounding Lee's explanation, it is evident that the flux of CO_2 from the air column below the instrument may be underestimated and hence measured NEE is overestimated. Hence the model's slight underestimates of observed nighttime NEE seen in Figure 4d may be reasonable. Conversely, the model evidently overestimates daytime NEE, which implies either that ecosystem respiration is underestimated or that net photosynthesis is also exagger-

ated. The simulation of net photosynthesis is derived from the Farquhar-Collatz model, however, which assumes simultaneous stomatal regulation of CO_2 exchange and transpiration. The strong agreement between measured and modeled LE indicates that the photosynthetic flux is approximately correct, which therefore suggests more investigation of respiration processes within IBIS is warranted.

Another source of the nighttime respiration discrepancy could originate from the soil carbon density data reported by *Gower et al.* [1997], that were used to initialize the model, and which affect soil respiration. These data (see Table 5 of *Gower et al.* [1997]), are considerably lower than those reported by other investigators (e.g., T. Nerbus and D. Anderson, University of Saskatchewan, unpublished data, 1996; H. Veldius, University of Manitoba, unpublished data, 1996). A higher value of initial soil carbon content would result in greater simulated soil respiratory fluxes during the growing season, assuming all other factors are unchanged. A sensitivity test showed, however, that even if the higher value of initial soil carbon was used, it could not provide a complete explanation for the discrepancy obtained between measured and simulated midday NEE.

Over the entire simulation period (NEE-3 in Table 2), the model explained $\sim 96\%$ of NEE measured at SOA (original IBIS run). This overall agreement hides fairly serious discrepancies, however, in both summer and winter data sets. For the

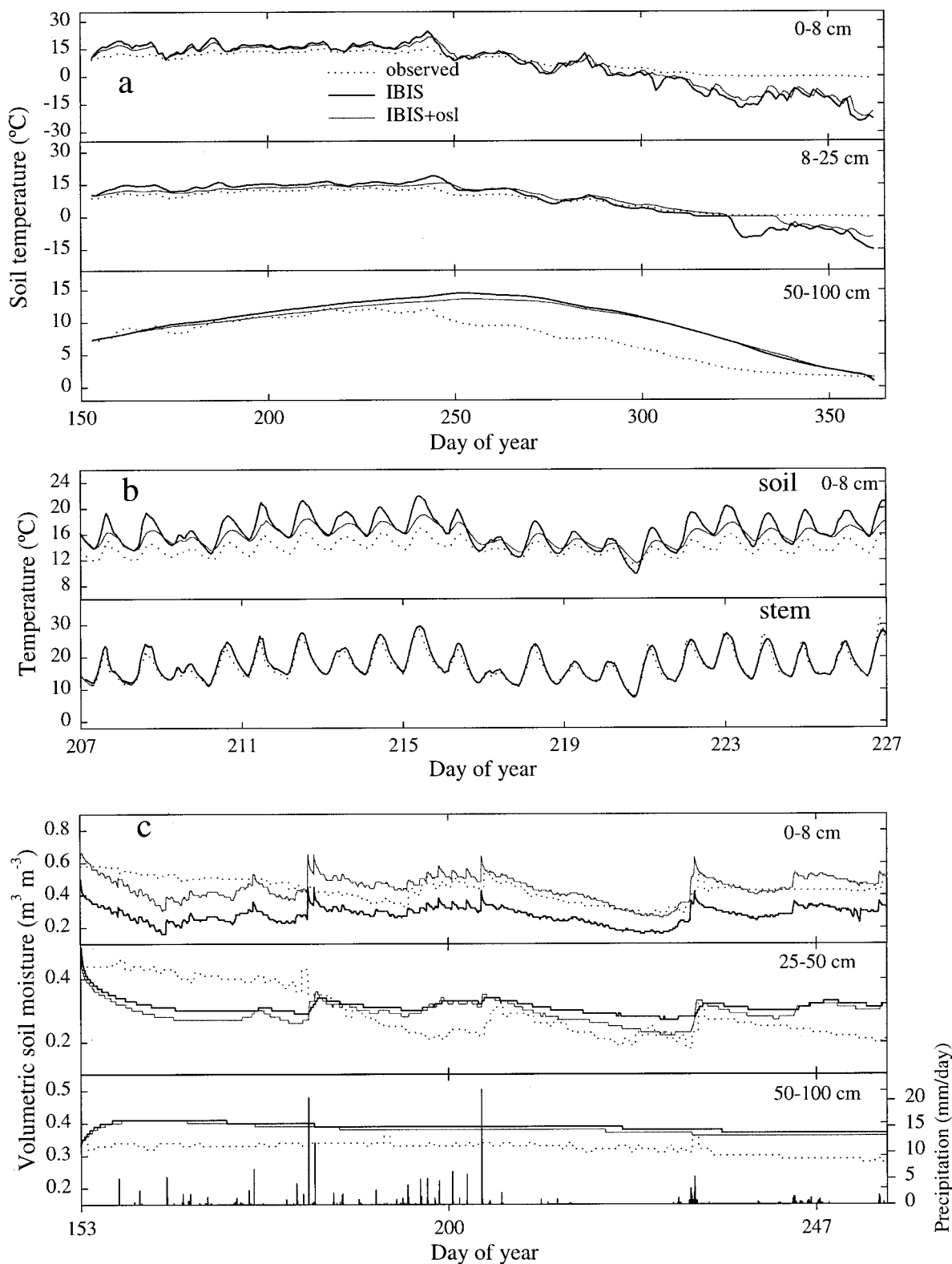


Figure 6. Observed and simulated: (a) daily soil temperature, (b) hourly soil and stem temperatures, and (c) daily soil moisture content, at old aspen site. Note that the horizontal scales differ significantly between Figures 6a, 6b, and 6c.

period when trees are in leaf and NEE indicates net carbon uptake (NEE-1 in Table 2), the ratio of observed to modeled NEE is ~ 0.81 , compared to ~ 0.54 for the period when trees are leafless and NEE indicates net carbon release (NEE-2 in

Table 2). Simulated wintertime CO₂ efflux is generally much higher than it should be, suggesting that the temperature response of the soil respiration model is too shallow.

While including the OSL substantially improved the simu-

lation of G , turbulent fluxes (H and LE) were virtually unchanged (Figures 3a–3d, 4a, 4b, and Table 2). Average NEE increased by $\sim 10\%$ in response to the simulated OSL, although this response was restricted almost entirely to the growing season (Table 2). The explanation for this appears to be that the organic layer increased water infiltration and reduced runoff, thereby increasing soil surface water availability (Figure 6c) and reducing vegetation drought stress. This in turn led to a reduction in the seasonal constraints on vegetation-atmosphere exchanges of water and carbon.

The model was able to reproduce stem temperature successfully (Figure 6b), whereas soil temperature was generally overestimated, but particularly in the topmost soil layer. This was due partly to the inconsistencies in the numerical solution of skin temperature mentioned previously. Adding the OSL to the original model resulted in greater soil moisture content in the top soil layer, however, which led to increased heat capacity and decreased soil surface soil temperature (Figures 6a and 6b). It should be borne in mind, however, that the results obtained from the IBIS + osl run are dependent on the value estimated for the saturated hydraulic conductivity of the organic layer (see section 4). Moreover, the observations did not show any significant soil moisture increase in response to the high rainfall (~ 60 mm) recorded on Julian days 188 and 189 (Figure 6c), which suggests a problem in data acquisition during this period.

Temperature of the 50–100 cm soil layer was also overestimated by the simulation between days 250 and 350. This suggests poor representation of heat diffusion to deep soil after the latter reached its peak temperature in the summer.

5.2. SYA Site

Reasonable agreement between simulated and observed fluxes of R_n and LE was obtained, although R_n was slightly underestimated during nighttime (Figures 7a, 7b, 7e, and 7f). In general, H was overestimated, but particularly at night (Figures 7c and 7d; see also Table 2). This nighttime exaggeration could be due to simulated release of heat stored in the canopy during the day. Daily stored energy is also likely to be partly released in the form of evaporation of water at night (Figure 7f). These nighttime releases would then cause, in turn, a systematic underestimation of nighttime R_n for the SYA site (Figure 7b) as well for the other sites (Table 2). Figure 7d also shows that the diurnal course of simulated H generally lagged the observational data. As reported above, this originates from the delayed transfer of soil temperature information into the atmospheric boundary layer calculations. Nevertheless, as with the SOA site, simulating an organic surface layer caused a significant improvement in modeled soil heat flux, both tightening the distribution of points and shifting the regression slope closer to the 1:1 line (Figures 7g and 7h).

5.3. SOJP Site

R_n was simulated correctly during the day but underestimated at night (Figures 7a and 7b; diurnal cycle is not shown (see section 5.2. for illustration)). As for the deciduous forest sites (SOA and SYA), LE was generally better simulated than H (Figures 8c–8f). The disagreement between observed and simulated H around midday was smaller, however, than at the deciduous forest sites. The existence of measured data on canopy heat storage for this site allows verification of the explanation given in section 5.1 concerning underestimation of

midday H by the model. Figure 9 shows clearly that when energy received by the surface was close to maximum, the simulated canopy heat storage could exceed 100 W m^{-2} . Conversely, during the night the model simulated greater release of stored energy than observed (Figure 9), causing H to be overestimated (Figures 8c and 8d). Introducing the OSL produced no significant improvement in simulated H and LE fluxes, although G was substantially improved and to a greater extent than at the deciduous sites (Figures 8g and 8h).

The largest discrepancy between measured and simulated NEE was also obtained around midday (Figures 8i and 8j; diurnal cycle not shown). Nighttime respiration was correctly simulated, however, which supports the hypothesis that the simulation of temperature effects on canopy respiration, during daylight periods in both coniferous and deciduous ecosystems, requires further modelling effort.

Soil temperature was generally exaggerated by the model at this site (Figure 10). Furthermore, the discrepancy between observed and simulated soil temperatures increased with depth, suggesting that soil thermal diffusivity was significantly lower in reality than implied by the values used in the model. This conclusion was confirmed by simulating the OSL, which improved agreement for the upper soil layers (depths to 25 cm), but still resulted in appreciable overestimation of average temperatures.

5.4. NOBS Site

In the northern boreal region, soil organic layers are typically deeper than 50 cm [Clayton *et al.*, 1977]. Hence, for the NOBS site located in the BOREAS-NSA, thickness of the OSL was set to 50 cm for the IBIS + osl run, corresponding to the top three soil layers in IBIS. Porosity, field capacity, and wilting point data (in terms of volumetric water content) were taken from Nijssen *et al.* [1997] (Table 1). The standard IBIS run, i.e., assuming only mineral soil at the surface was carried out using a silty clay soil texture, corresponding to that used in IBIS for global simulations (see section 3).

As with the other sites, observed R_n was simulated better for daytime than nighttime (Figures 11a and 11b). Including the organic layer resulted in almost no changes in simulated H (Figures 11c and 11d), but produced significantly better prediction of LE (Figures 11e and 11f). The major contributing factor for the improvement in LE was the reduction of G (Table 2; note that measurements of G were not available for this site), which resulted from the greater moisture storage capacity in the 50 cm OSL, compared to the lower porosity of the mineral layers. Comparison of observed and simulated mean Bowen ratios for this site and for OJP shows that both are greater than 1.0 (Table 2), whereas those for the deciduous sites were typically much lower.

According to the Collatz [1991, 1992] model used in IBIS, changes in stomatal conductance to water vapour lead directly to changes in CO_2 uptake. The improvements in LE resulting from including the OSL in the NOBS simulations therefore also appear to contribute to improved simulation of NEE, with both a higher mean and a wider range between minimum and maximum values (Figures 11g and 11h). As with the SOA and SOJP sites, however, NEE values around midday were overestimated. When integrated over the whole period, the total simulated NEE indicates a slight carbon source when no organic layer is included (Table 2), compared to an observed net sink for the measurement period. In the IBIS + osl simulation,

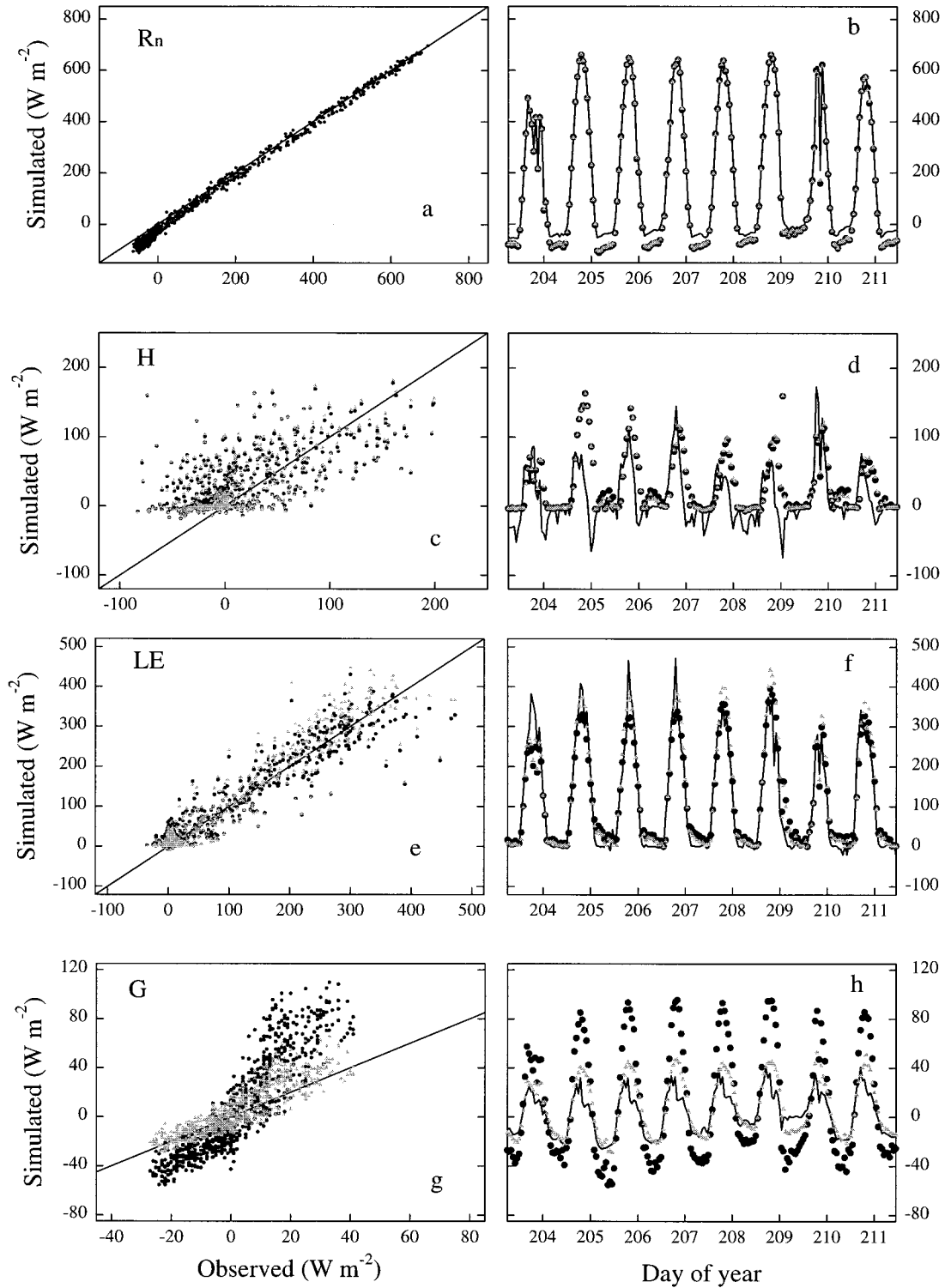


Figure 7. Simulated hourly above-canopy fluxes plotted against data observed at the young aspen site during the period July 17 to August 16, 1994. (a, b) Net radiation. (c, d) Sensible heat flux. (e, f) Latent heat flux. (g, h) Soil heat flux. Dark dots indicate assumed presence of mineral soil only; light triangles indicate assumed presence of mineral soil with surface organic layer.

however, the inclusion of an organic layer resulted in an average net sink, comparable in magnitude to the observed value.

Agreement between observed and simulated soil temperatures for the top layer also improved when the OSL was con-

sidered (Figure 12), but with increasing depth, this agreement became progressively poorer. Inclusion of the OSL also improved the timing of the onset of soil thawing at the topmost layer.

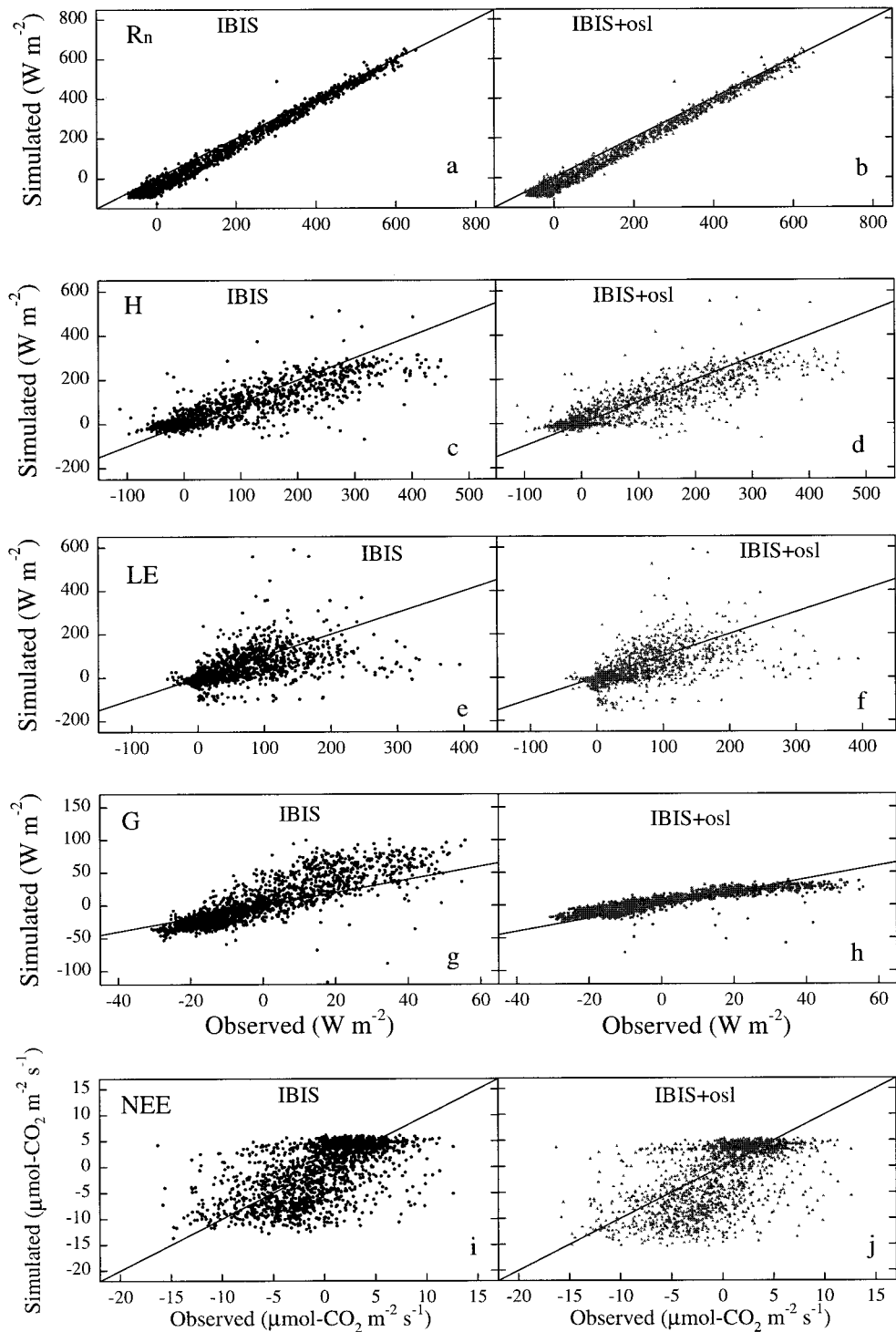


Figure 8. Simulated hourly above-canopy fluxes plotted against data observed at the old jack pine site during the period July 1 to September 16, 1994. (a) Net radiation assuming presence of mineral soil only, (b) mineral soil with surface organic layer. (c) Sensible heat flux assuming presence of mineral soil only, (d) mineral soil with surface organic layer. (e) Latent heat flux assuming presence of mineral soil only, (f) mineral soil with surface organic layer. (g) Soil heat flux assuming presence of mineral soil only, (h) mineral soil with surface organic layer. (i) Net ecosystem exchange (NEE) assuming presence of mineral soil only, (j) mineral soil with surface organic layer. Carbon flux (NEE) is positive toward the atmosphere.

6. Discussion and Conclusions

Collective understanding of the physical, physiological, and ecological processes governing terrestrial biospheric behavior

has increased significantly over the last 30 years. As this understanding has developed, so too has the desire to encapsulate it in simulation models of increasing complexity. Current-generation biospheric models such as IBIS are highly

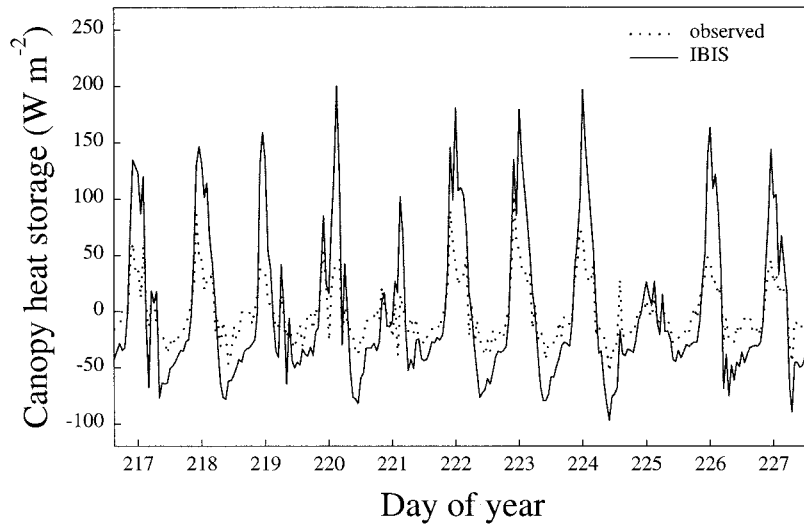


Figure 9. Illustration of diurnal variation of observed (dotted line) and simulated (original IBIS; solid line) canopy heat storage at old jack pine site during summer.

sophisticated, but this sophistication also makes them very difficult to test. In order to have confidence in such models, e.g., when using them to investigate effects of future environmental changes on the biosphere, it is essential to test and

validate them against observed data at the local (site-level) scale as well as at the continental and global scales. Hence, as a part of a project to explore climate change effects on Canada's forests, this study compared IBIS version 2.1 with data

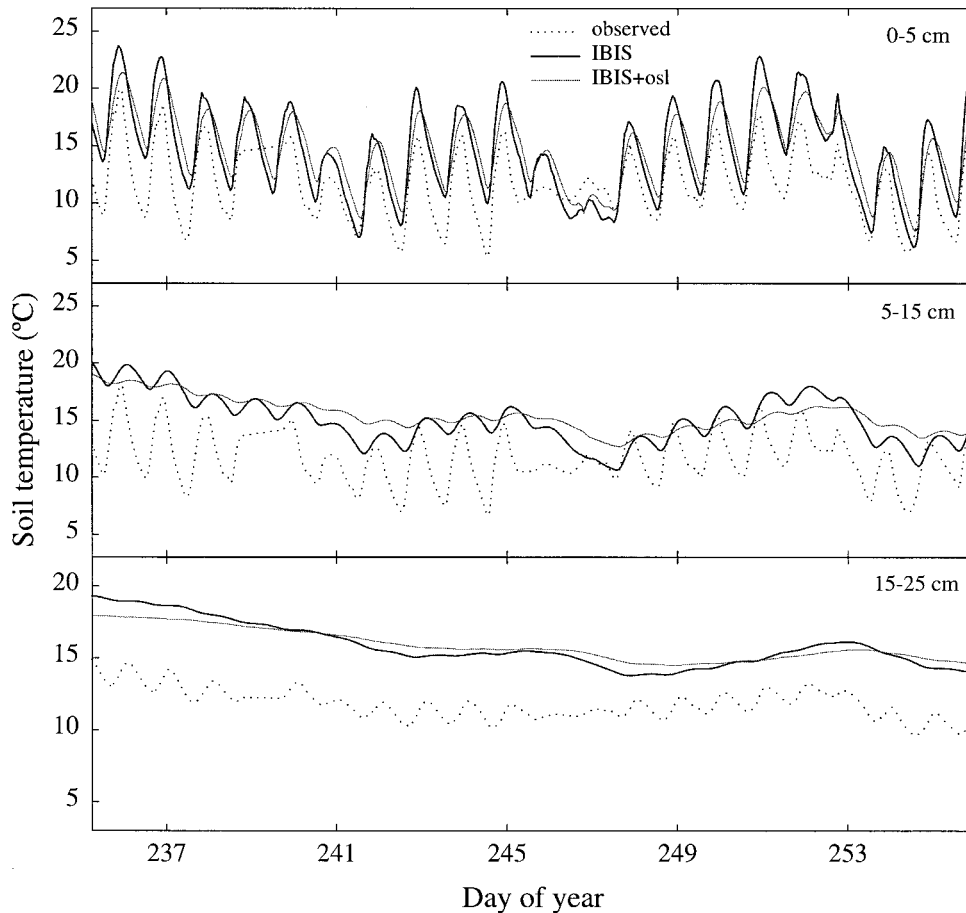


Figure 10. Observed (dotted line) and simulated diurnal variation of soil temperature at old jack pine site. Bold solid line indicates assumed presence of mineral soil only; thin solid line indicates assumed presence of mineral soil with surface organic layer.

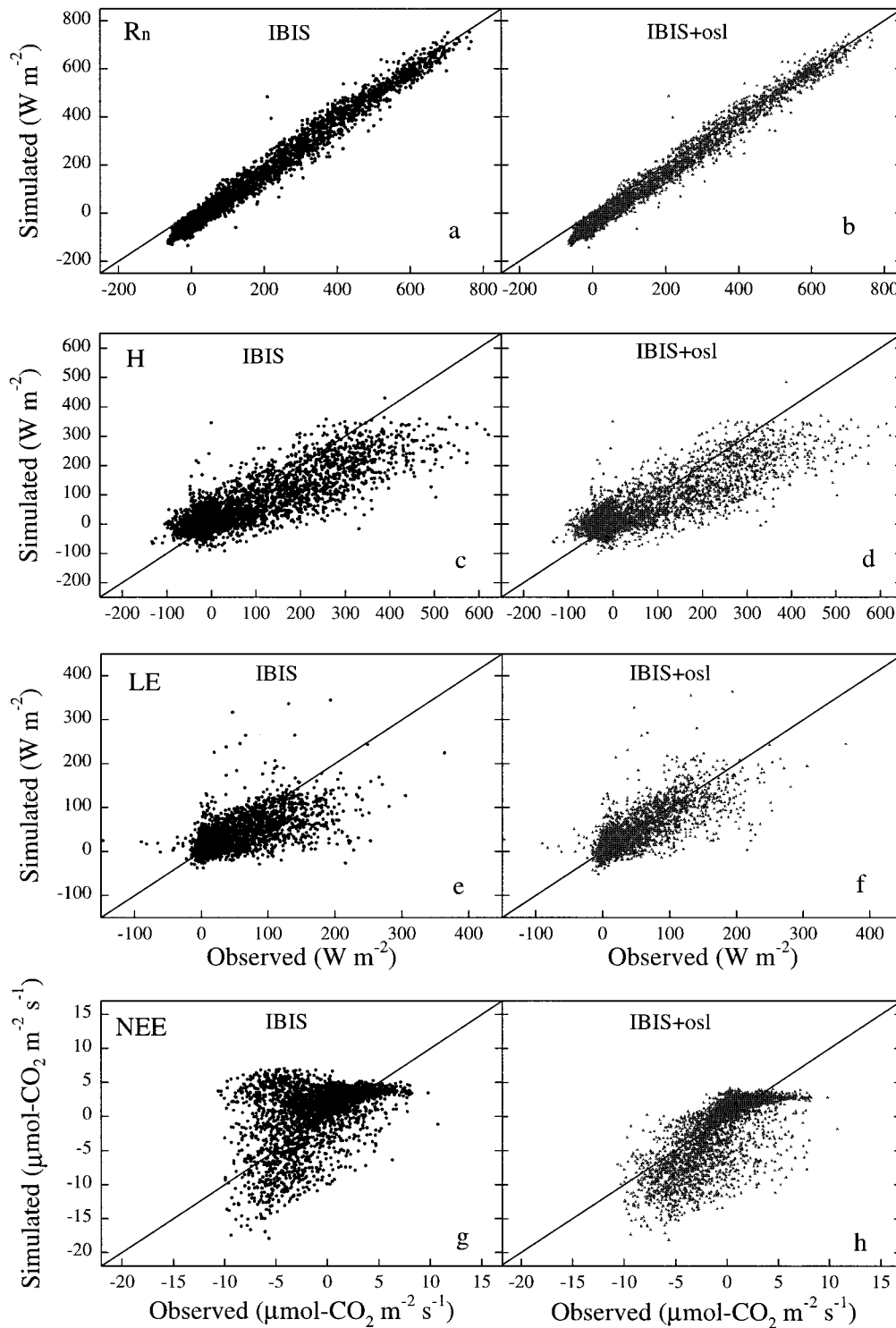


Figure 11. Simulated hourly above-canopy fluxes plotted against data observed at the old jack pine site during the period April 1 to October 9, 1996. (a) Net radiation assuming presence of mineral soil only, (b) mineral soil with surface organic layer. (c) Sensible heat flux assuming presence of mineral soil only, (d) mineral soil with surface organic layer. (e) Latent heat flux assuming presence of mineral soil only, (f) mineral soil with surface organic layer. (g) Net ecosystem exchange (NEE) assuming presence of mineral soil only, (h) mineral soil with surface organic layer. Carbon flux (NEE) is positive toward the atmosphere.

from different boreal forest types obtained in the BOREAS experiment.

The results showed both successes and deficiencies in IBIS' ability to simulate exchanges of mass and energy over boreal

ecosystems. Although evapotranspiration was generally simulated reasonably well, sensible heat fluxes were systematically underestimated. The latter problem was more evident at a mature deciduous forest site (SOA) than at coniferous sites

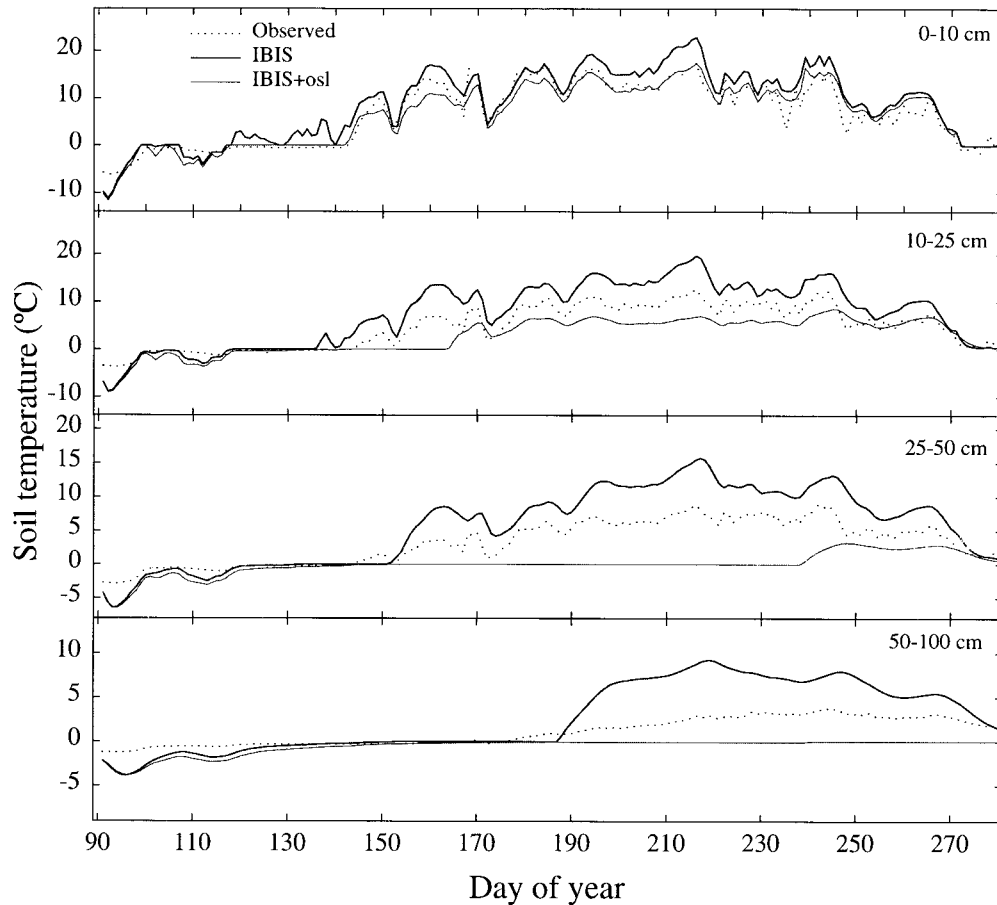


Figure 12. Observed (dotted line) and simulated daily soil temperature at old black spruce site. Thick solid line indicates assumed presence of mineral soil only; thin solid line indicates assumed presence of mineral soil with surface organic layer.

(SOJP and NOBS). A sensitivity test and comparison with measured canopy heat storage data showed that this problem could be related to the physical parameterizations used to represent heat transfer between vegetation and atmosphere. Evidently, further work is required to improve the representation of canopy heat storage in the model.

Net ecosystem exchange of carbon (NEE) was generally simulated acceptably, although for the SOA site, summer and winter estimates showed appreciable bias compared to the means of all data (see Table 2). Furthermore, midday assimilation was generally overestimated, which appears to be due to underestimation of daytime respiration rates. The origin of this problem is not easy to determine: it could result from underestimation of soil respiration temperature coefficients (we do not have measured soil respiration data), or it could be due to underestimating soil carbon content (see above, section 5.1.). Future analyses based on field measurements are required. Careful validation of the soil biogeochemistry component of IBIS against extensive field measurements of soil respiration should help to resolve this problem.

Simulated ecosystem respiration was also evidently overestimated during the winter period at SOA. This, combined with a general tendency to overestimate nighttime respiration, may suggest that the temperature responses for respiration (of soil and/or vegetation) are too shallow. Furthermore, for a better evaluation of NEE simulated by such DGVMs, more complete

understanding is needed of the problems in using eddy correlation over tall canopies at nighttime when wind speeds are low, available energy is small and atmospheric stability is high [e.g., Lee, 1998; Baldocchi *et al.*, 1998]. Hence it is to be expected that the model can be further improved as technical measurement problems are resolved or alternative techniques are developed.

Both observed and simulated mean Bowen ratios for coniferous sites (SOJP and NOBS) were greater than 1.0, whereas those for the deciduous sites were typically much lower. This demonstrates that IBIS is able to reproduce correctly one of the fundamental differences between deciduous and conifer-dominated boreal ecosystems. The importance of predicting these differences in the Bowen ratio successfully is related to the influence of H and LE on mesoscale and local weather conditions (see the review of Pielke *et al.* [1998] and Hogg *et al.* [2000]). This implies that IBIS simulations of changes in vegetation, e.g., due to global warming effects on species competition and physiology, will lead to changes in the surface fluxes used as lower boundary conditions when IBIS is coupled to a GCM.

The results of this study also showed the importance of including an organic layer in simulating surface energy carbon fluxes for boreal forest stands. The presence of surface organic material affects soil moisture and temperature, as well as soil heat flux, soil thawing, surface energy partitioning, and sur-

face-atmosphere carbon exchange. For instance, inclusion of the OSL in the model led to appreciable improvements in simulated soil heat flux and surface temperature, providing an additional explanation for why existing land surface models tend to overestimate soil “skin” temperature and downward soil heat flux. *Betts et al.* [1993] and *Chen et al.* [1997] related this problem to the numerical algorithms adopted to solve the surface energy balance (see also *Beljaars* [1991] for numerical details). Results for soil temperature at the NOBS site also showed that the inclusion of a surface organic layer delays the start of thawing, which in turn affects soil moisture availability, although it is clear that with increasing depth, the simulation of this delay is much less satisfactory (see Figure 12d). This effect is of considerable interest because several studies have demonstrated the importance of correct estimation of soil moisture content on the Bowen ratio, which in turn affects the development of the atmospheric boundary layer, and hence both local and regional atmospheric conditions (an extensive review can be found in the work of *Betts et al.* [1996]). Moreover, *Goulden et al.* [1998] showed the importance of soil depth and thaw on boreal forest carbon balance. It will be particularly important in spatial modeling therefore that the physical characteristics of both mineral and organic soil layers be properly parameterized. In order to achieve this difficult goal a starting point could be to test land surface parameterizations at a range of sites, using measured data for the vertical distributions of soil texture, soil thermal and hydraulic properties, soil carbon content, and root biomass. Unfortunately, extensive data sets containing reliable values for these variables are not generally available. Future field campaigns should attempt to report such information, as suggested also by *Delire and Foley* [1999]. For instance, some of the disagreement between observed and simulated soil temperature and moisture, and hence energy and carbon fluxes, obviously originates from the use of a constant soil texture profile in our simulations. Concerning surface organic material, *Enrique et al.* [1999] attempted to quantify the effect of plant-residue mulch on energy exchange between a grassland ecosystem and the atmosphere. A comparable, physically based, approach could be developed for forest canopies, but for organic material in varying states of decomposition.

The importance of these effects of the organic surface layer on simulated exchanges of water and carbon is, of course, dependent upon its thickness. This study shows that consideration of the OSL in the model has only a minor effect on simulated water and carbon fluxes, for both deciduous and coniferous sites where the organic material thickness does not exceed a few centimetres. For the northern black spruce site, however, where the organic layer is 50 cm thick, the simulation of both latent heat flux and NEE were substantially improved when this was taken into consideration in the model.

This study confirms and builds upon similar work by *Delire and Foley* [1999] who applied IBIS to other vegetation types including grassland and tropical forest ecosystems. Such studies help to confirm the validity of the process components of IBIS and hence its value as a global ecosystem simulator. Although other aspects of the model still require validation, e.g., competition and phenology, validations such as ours have two major benefits. First, they increase confidence that the use of dynamic vegetation simulators will improve the representation of land surface effects when coupled to GCMs, and hence allow climate modelers to improve predictions of how vegetation feedbacks may affect climate as the climate changes. Sec-

ond, they provide a very good basis for estimating the probable errors in simulations of canopy exchange processes at regional and global scales.

Acknowledgments. We thank ENergy from the FOREst (ENFOR), funded by the Canadian Federal Panel on Energy Research and Development (PERD), who provided the financial support of this study. Brian Amiro, Robert Grant, Ted Hogg, and three anonymous reviewers provided careful reviews of an earlier version of this manuscript. AMS mesonet data were provided by the Saskatchewan Research Council. We wish to thank M. Goulden and D. Baldocchi for making, respectively, NOBS and SOJP data available to the BOREAS research community.

References

- Baldocchi, D. D., C. A. Vogel, and B. Hall, Seasonal variation of carbon dioxide exchange rates above and below a boreal jack pine forest, *Agric. For. Meteorol.*, **83**, 147–170, 1997a.
- Baldocchi, D. D., C. A. Vogel, and B. Hall, Seasonal variation of energy and water vapor exchange rates above and below a boreal jack pine forest, *J. Geophys. Res.*, **102**(D24), 28,939–28,952, 1997b.
- Baldocchi, D., K. Wilson, and K. T. Paw U, On measuring net ecosystem carbon exchange in complex terrain over tall vegetation, paper presented at 23rd Conference on Agricultural and Forest Meteorology, Nov. 2–6, Am. Meteorol. Soc., Albuquerque, N. M., 1998.
- Ball, J. T., I. E. Woodrow, and J. A. Berry, A model predicting stomatal conductance and its contribution to the control of photosynthesis under different environmental conditions, in *Progress in Photosynthesis Research*, vol. 4, edited by J. Biggins, pp. 221–224, Martinus-Nijhoff, Zoetermeer, Netherlands, 1986.
- Beljaars, A. C. M., Numerical schemes for parameterizations, in *Numerical Methods in Atmospheric Models*, vol. 11, pp. 1–42, Eur. Cent. for Medium Range Weather Forecasts, Reading, England, Sept. 1991.
- Bellisario, L. M., L. D. Boudreau, D. L. Verseghy, W. R. Rouse and P. D. Blanken, Comparing the performance of the Canadian Land Surface-Scheme (CLASS) for two subarctic terrain types, *Atmos. Ocean*, **38**(1), 181–204, 2000.
- Bessemoulin, P., and D. Puech, BOREAS TF-06 SSA-YA Surface energy flux and meteorological data, <http://www.eodis.ornl.gov/>, Distrib. Active Archive Cent., Oak Ridge Laboratory, Oak Ridge, Tenn., 1998.
- Betts, A. K., J. H. Ball, and A. C. Beljaars, Comparison between the land surface response of the European Centre Model and the FIFE-1987 data, *Q.J.R. Meteorol. Soc.*, **119**, 975–1001, 1993.
- Betts, A. K., J. H. Ball, A. C. Beljaars, M. J. Miller, and P. Viterbo, The land-surface-atmosphere interaction: A review based on observational and global modeling perspectives, *J. Geophys. Res.*, **101**(D3), 7209–7225, 1996.
- Black, T. A., and Z. Nestic, Boreal forest atmosphere interactions: Exchanges of energy, water vapor and traces gases, Distrib. Active Archive Cent., Oak Ridge Natl. Lab., Oak Ridge, Tenn., 1998. (Available at <http://www.eodis.ornl.gov/>)
- Black, T. A., G. Den Hartog, H. H. Neumann, P. D. Blanken, P. C. Yang, C. Russell, Z. Nestic, X. Lee, S. G. Chen, R. Staebler, and M. D. Novak, Annual cycles of water vapour and carbon dioxide fluxes in and above a boreal aspen forest, *Global Change Biol.*, **2**, 159–168, 1996.
- Bonan, G. B., D. Pollard, and S. L. Thompson, Effects of boreal forest vegetation on global climate, *Nature*, **359**, 716–718, 1992.
- Brutsaert, W., *Evaporation into the Atmosphere*, 299 pp., D. Reidel, Norwell, Mass., 1982.
- Calvet, J. C., J. Noilhan, J.-L. Roujean, P. Bessemoulin, M. Cabelluene, A. Olioso, and J.-P. Wigneron, An interactive vegetation SVAT model tested against data from six contrasting sites, *Agric. For. Meteorol.*, **92**, 73–95, 1998.
- Campbell, G. S., and J. M. Norman, *An Introduction to Environmental Biophysics*, 286 pp., Springer-Verlag, New York, 1998.
- Chen, T. H., et al., Cabauw Experimental results from the Project for Intercomparison of Land-surface Parameterization Schemes, *J. Clim.*, **10**, 1194–1215, 1997.
- Chen, W. J., et al., Effects of climatic variability on the annual carbon

- sequestration by a boreal aspen forest, *Global Change Biol.*, *5*, 41–53, 1999.
- Ciais, P., P. Tans, M. Trolier, J. White, and R. Francey, A large Northern Hemisphere terrestrial CO₂ sink indicated by ¹³C/¹²C ratio of atmospheric CO₂, *Science*, *269*, 1098–1102, 1995.
- Clayton, J. S., W. A. Ehrlich, D. B. Cann, J. H. Day, and I. B. Marshall, *Soils of Canada*, vol. 2, *Inventory*, 239 pp., Res. Branch, Can. Dep. of Agric., Ottawa, Ontario, 1977.
- Collatz, G. J., J. T. Ball, C. Grivet and J. A. Berry, Physiological and environmental regulation of stomatal conductance, photosynthesis and transpiration: A model that includes a laminar boundary layer, *Agric. For. Meteorol.*, *53*, 107–136, 1991.
- Collatz, G. J., M. Ribas-Carbo, and J. A. Berry, Coupled photosynthesis-stomatal conductance model for leaves of C₄ plants, *Aust. J. Plant Physiol.*, *19*, 519–538, 1992.
- Cuenca R. H., D. E. Strangel, and S. F. Kelly, Soil water balance in a boreal forest, *J. Geophys. Res.*, *102*(D24), 29,355–29,367, 1997.
- Delire, C., and J. A. Foley, Evaluating the performance of a land surface/ecosystem model with biophysical measurements from contrasting environments, *J. Geophys. Res.*, *104*(D4), 16,895–16,909, 1999.
- Dickinson, R. E., A. Henderson-Sellers, P. J. Kennedy, M. F. Wilson, Biosphere-Atmosphere Transfer Scheme (BATS) for the NCAR CCM, *Tech. Note NCAR/TN-275-STR*, Natl. Cent. for Atmos. Res., 69 pp., Boulder, Colo., 1986.
- Enrique, G.-S., I. Braud, J.-L. Thony, M. Vauclin, P. Bessemoulin, and J.-C. Calvet, Modelling heat and water exchanges of fallow land covered with plant-residue mulch, *Agric. For. Meteorol.*, *97*, 151–169, 1999.
- Farquhar, G. D., S. von Caemmerer, and J. A. Berry, A biochemical model of photosynthetic CO₂ assimilation in leaves of C₃ species, *Planta*, *149*, 78–90, 1980.
- Foley, J. A., J. E. Kutzbach, M. T. Coe, and S. Levis, Feedbacks between climate and boreal forests during the holocene epoch, *Nature*, *371*, 52–54, 1994.
- Foley, J. A., I. C. Prentice, N. Ramankutty, S. Levis, D. Pollard, S. Sitch, and A. Haxeltine, An integrated biosphere model of land surface processes, terrestrial carbon balance, and vegetation dynamics, *Global Biogeochem. Cycles*, *10*(4), 603–623, 1996.
- Gates, D. M., *Plant-Atmosphere Relationships*, 92 pp., Chapman and Hall, New York, 1993.
- Goulden, M. L., B. C. Daube, S. M. Fan, D. J. Sutton, A. Bazzaz, J. W. Munger, and S. C. Wofsy, Physiological responses of a black spruce forest to weather, *J. Geophys. Res.*, *102*(D24), 28,987–28,996, 1997.
- Goulden, M. L., et al., Sensitivity of boreal forest carbon balance to soil thaw, *Science*, *279*, 214–217, 1998.
- Gower, S. T., J. G. Vogel, J. M. Norman, C. J. Kucharik, S. J. Steele, and T. K. Stow, Carbon distribution and aboveground net primary production in aspen, jack pine, and black spruce stands in Saskatchewan and Manitoba, Canada, *J. Geophys. Res.*, *102*(D24), 29,029–29,041, 1997.
- Guyot, G., *Climatologie de l'Environnement*, 505 pp., Masson, Paris, 1997.
- Henderson-Sellers, A., and V. B. Brown, Project of the Intercomparison of Land-surface Parameterization Schemes (PILPS): First science plan, *IGPO Publ. Ser.*, vol. 5, 53 pp., 1992.
- Henderson-Sellers, A., K. McGuffie, and A. J. Pitman, The project for Intercomparison of Land-surface Parameterization Schemes (PILPS): 1992 to 1995, *Clim. Dyn.*, *12*, 849–859, 1996.
- Hogg, E. H., D. T. Price, and T. A. Black, Postulated feedbacks of deciduous forest phenology on seasonal patterns in the western Canadian interior, *J. Clim.*, *13*(24), 4229–4243, 2000.
- Jackson, R. B., J. Canadell, J. R. Ehleringer, H. A. Mooney, O. E. Sala, and E. D. Schulze, A global analysis of root distribution for terrestrial biomes, *Oecologia*, *108*, 389–411, 1996.
- Kimball, J. S., P. E. Thornton, M. A. White, and S. W. Running, Simulating forest productivity and surface-atmosphere carbon exchange in the BOREAS study region, *Tree Physiol.*, *17*, 589–599, 1997.
- Kucharik, C. J., J. A. Foley, C. Delire, V. A. Fisher, M. T. Coe, J. Lenters, C. Young-Molling, N. Ramankutty, J. M. Norman, and S. T. Gower, Testing the performance of a dynamic global ecosystem model: Water balance, carbon balance and vegetation structure, *Global Biogeochem. Cycles*, *14*(3), 795–825, 2000.
- Larson, J. A., *The Boreal Ecosystem*, 500 pp., Academic, San Diego, Calif., 1980.
- Lee, X., On micrometeorological observations of surface-air exchange over tall vegetation, *Agric. For. Meteorol.*, *91*, 39–49, 1998.
- Loyd, J., and J. A. Taylor, On the temperature dependence of soil respiration, *Functional Ecol.*, *8*, 315–323, 1994.
- Manabe, S., and K. Bryan, Climate calculations with a combined ocean-atmosphere model, *J. Atmos. Sci.*, *26*, 786–789, 1969.
- Manabe, S., and R. T. Wetherald, Large-scale changes of soil wetness induced by an increase in atmospheric carbon dioxide, *J. Atmos. Sci.*, *44*, 1211–1235, 1987.
- Nijssen, B., I. Haddeland, and D. P. Lettenmaier, Point evaluation of a surface hydrology model for BOREAS, *J. Geophys. Res.*, *102*(D24), 29,367–29,378, 1997.
- Pielke, R. A., and P. L. Vidale, The boreal forest and the polar front, *J. Geophys. Res.*, *100*(D12), 25,755–25,758, 1995.
- Pielke, R. A., T. J. Lee, J. H. Copeland, J. L. Eastman, C. L. Ziegler, and C. A. Finley, Use of USGS-provided data to improve weather and climate simulations, *Ecol. Appl.*, *7*, 1053–1069, 1997.
- Pielke, R. A., R. Avissar, M. Raupach, A. J. Dolman, X. Zeng, and A. S. Denning, Interactions between the atmosphere and terrestrial ecosystems: Influence on weather and climate, *Global Change Biol.*, *4*, 461–475, 1998.
- Pollard, D., and S. L. Thompson, Use of a land-surface-transfer scheme (LSX) in a global climate model: The response to doubling stomatal resistance, *Global Planet. Change*, *10*, 129–161, 1995.
- Satterlund, D. R., An improved equation for estimating long-wave radiation from the atmosphere, *15*(6), 1649–1650, 1979.
- Schneider, S. H., and R. E. Dickinson, Climate modeling, *Rev. Geophys.*, *12*, 447–493, 1974.
- Sellers, P. J., Y. Mintz, Y. C. Sud, and A. Dalcher, A Simple Biosphere model (SiB) for use within general circulation models, *J. Atmos. Sci.*, *43*, 505–531, 1986.
- Sellers, P. J., D. A. Randall, G. J. Collatz, J. A. Berry, C. B. Field, D. A. Dazlich, C. Zhang, G. D. Collelo, and L. Bounoua, A revised land surface parameterization (SiB2) for atmospheric GCMs, part I, Model formulation, *J. Clim.*, *9*(4), 676–705, 1996.
- Sellers, P. J., et al., BOREAS in 1997: Experiment overview, scientific results, and future directions, *J. Geophys. Res.*, *102*(D24), 28,731–28,769, 1997.
- Shao, Y., and A. Henderson Sellers, Modeling soil moisture: A project for Intercomparison of Land Surface Parameterization Schemes Phase 2(b), *J. Geophys. Res.*, *101*(D3), 7227–7250, 1996.
- Shewchuk, S. R., Surface mesonet for BOREAS, *J. Geophys. Res.*, *102*(D24), 29,077–29,082, 1997.
- Shukla, J., and Y. Mintz, Influence of land-surface evapotranspiration on the Earth's climate, *Science*, *215*, 1498–1501, 1982.
- Steele, S. J., S. T. Gower, J. G. Vogel, and J. M. Norman, Root mass, net primary production and turnover in aspen, jack pine and black spruce forests in Saskatchewan and Manitoba, Canada, *Tree Physiol.*, *17*, 577–587, 1997.
- Tans, P. P., I. Y. Fung, and T. Takahashi, Observational constraints on the global atmospheric CO₂ budget, *Science*, *247*, 1431–1438, 1990.
- Verma, S. B., J. Kim, and R. J. Clement, Momentum, water vapor, and carbon dioxide exchange at a centrally located prairie site during FIFE, *J. Geophys. Res.*, *97*, 18,629–18,639, 1992.
- Verseghy, D. L., N. A. McFarlane, and M. Lazare, CLASS-A Canadian land surface scheme for GCMs, II, Vegetation model and coupled runs, *Int. J. Climatol.*, *13*, 347–370, 1993.

P. Bessemoulin, Météo-France, Service Central d'Exploitation de la Météorologie, 42 Avenue G. Coriolis, 31057 Toulouse Cédex, France.
A. Black, Department of Agroecology, University of British Columbia, Vancouver, BC, Canada V6T 1Z4.

C. Delire and J. A. Foley, Center for Sustainability and the Global Environment, Institute for Environmental Studies, University of Wisconsin, 1225 West Dayton Street, Madison, WI 53706.

M. El Maayar and D. T. Price, Natural Resources Canada, Canadian Forest Service, 5320-122 Street, Edmonton, AB, Canada T6H 3S5. (elmaayar@nrcan.gc.ca)

(Received May 31, 2000; revised February 20, 2001; accepted February 27, 2001.)

